Uranium Adsorption Characteristics of a Circulating Fluidized-Bed Adsorber

Yoshiro Ito, Susumu Nakamura, Masataka Shirakashi, and Masayoshi Kanno
Dept. of Mechanical Engineering, Nagaoka University of Technology, Nagaoka, Niigata 940-21, Japan

A new type of fluidized bed, called a circulating fluidized-bed adsorber (CFBA), was developed for processing a large quantity of water with high efficiency. Its fluid mechanical characteristics are reported, as well as recovery of uranium from natural seawater using a small CFBA. Using hydrous titanium oxide, granulated with polyacrylonitrile (PAN-HTO), as an adsorbent, CFBA ran stably for six days, the period required for the adsorbent to collect a practical amount of uranium. To predict the uranium adsorption performance of a plant-size CFBA, a numerical model simulating the adsorption kinetics was developed. The result of the numerical calculation by the model was in good agreement with the experimental data.

Introduction

Concentration of uranium in seawater is extremely low at 3.3 ppb. The total volume of the world's oceans, however, contains about 4 billion tons of uranium. Since it is almost a thousandfold greater than the terrestrial uranium resources of reasonable concentrations, the uranium in seawater is attractive resources for a country like Japan, where domestic uranium resources are rare.

Some types of adsorption processing by granular and fiber adsorbents are considered to be the basis of the uranium recovery system (Kanno, 1984). To recover significant amounts of uranium, an enormous volume of seawater must be contacted with the adsorbent because of the low concentration of uranium in seawater. Even if we assume 100% recovery efficiency, 3×10^{11} m^3/yr of seawater must be processed in an adsorption plant to recover one thousand tons of uranium a year.

Conventional contacting beds such as a fixed bed or a fluidized bed, however, cannot operate at a high seawater velocity. In these contacting beds, a linear velocity of seawater is limited to about 1 cm/s (Koske and Ohlrogge, 1983), because a high water velocity causes clogging and increases pressure drop in the fixed bed and the carryover of the adsorbent particles in the fluidized bed. The limit velocity of 1 cm/s corresponds to 1/2-1/4 of the settling velocity of an inorganic adsorbent particle. Therefore, the adsorption plant using such contacting beds needs a large adsorption bed area and becomes a huge plant.

Our previous study on the cost estimation for the fixed-bed system (Nakamura et al., 1987) showed that the major cost associated with an uranium production resulted from the construction of the adsorption facility. Thus, producing uranium by conventional contacting beds is not economical. New contacting devices that overcome deficiencies of conventional fixed- and fluidized-bed contactors are urgently needed. For this purpose, we developed a new type of fluidized bed, called a circulating fluidized-bed adsorber (CFBA) (Nakamura et al., 1990). CFBA consists of two rectangular pipes separated by a vertical partition wall. The two pipes, one which acts as a riser and the other as a downcomer, are interconnected at the top and the bottom.

In this study, the recovery of uranium from natural seawater was carried out using a small CFBA to investigate its adsorption characteristics. Hydrous titanium oxide granulated with polyacrylonitrile (PAN-HTO) was used as an adsorbent. CFBA ran stably with small loss of adsorbent over the period required by the adsorbent to collect a practical amount of uranium. Neither clogging nor change of the flow rate occurred during the period even when unfiltered seawater was supplied to CFBA. To predict the uranium adsorption performance of a plant-size CFBA, a numerical model simulating the adsorption kinetics in the CFBA was developed. The result of the numerical calculation by the model was in good agreement with the experimental data.

Correspondence concerning this article should be addressed to Y. Ito.

Experimental Studies

Outline of CFBA

Figure 1 shows CFBA used in the experiments, whose principle was previously described (Nakamura et al., 1990) and is only briefly outlined here. Water fed into the vessel from a nozzle (water inlet) develops a jet along the horizontal bottom wall and mixes with the adsorbent particles falling through a slit (particle nozzle) from the packing section. The jet of the mixture turns its direction upward and ascends in the contacting section. At the top of this section, the mixture overflows the partition wall and flows down toward the packing section. In the upper part of the packing section, the mixture collides with the surface of the packed adsorbent. Then, the particles deposit on the surface and gradually move downward to mix again with fresh seawater, while depleted water flows out of the opening on the top wall (water outlet). The major portion of the total pressure drop through the CFBA occurs in the contacting section, where the pressure drop is proportional to the amount of adsorbent suspended in it (Nakamura et al., 1990). In CFBA, no distributor is required to hold the adsorbent particles. Thus, the overall pressure drop is smaller in CFBA than that in conventional fluidized beds.

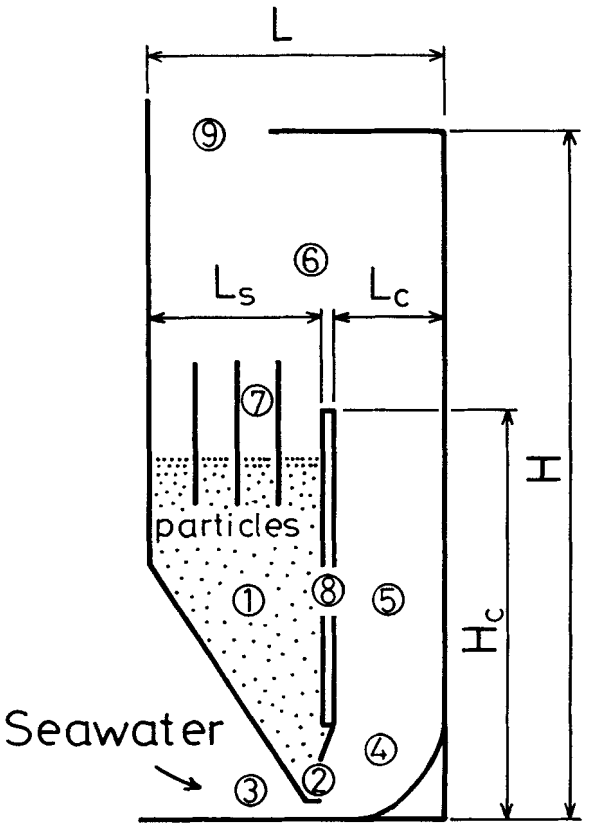

Figure 1. Circulating fluidized-bed adsorber.

1 = packing section
2 = particle nozzle
3 = water inlet
4 = mixing section
5 = contacting section
6 = sedimentation section
7 = baffle plates
8 = partition wall
9 = water outlet

Dimensions of the CFBA used in the experiments were: $H=25$ cm, $H_c=15$ cm, $L=10$ cm, $L_c=4$ cm, $L_s=5.5$ cm, and $T=5$ cm. The adsorbent inventory was 275 cm^3 and kept to 24% of the bed volume.

The CFBA used in the experiments had total bed height $H=25$ cm, contacting section height $H_c=15$ cm, bed width $L=10$ cm, contacting section width $L_c=4$ cm, packing section width $L_s=5.5$ cm, and bed thickness $T=5$ cm.

Adsorption experiment

Experiments on the adsorption of uranium from natural seawater were carried out at Sado Marine Biological Station of Niigata University located on the northern coast of Sado Island in the Japan Sea. Seawater temperature and solids suspended in seawater changed seasonally, so the adsorption experiments were conducted in three different seasons to examine these influences on the uranium uptake: in the middle of May, late in August, and early in November. The adsorption period of each experiment was six days. In our previous batch experiments (Nakamura et al., 1988), the concentration of uranium in the adsorbent reached equilibrium with that in the seawater after seven to nine days. Therefore, a practical amount of uranium could be collected within six days.

In the adsorption experiment shown in Figure 2, natural seawater was pumped into a 60-L overflow tank and supplied to the CFBA. Seawater was filtered to remove particulates larger than 10 μm for the first two seasons. In the November experiment, however, unfiltered seawater was supplied directly to the CFBA.

To simulate the uranium adsorption performance numerically, we need an intraparticle diffusion coefficient of uranium ion in the adsorbent particle. This coefficient is evaluated by comparing the experimental uranium uptake curve in a column with theoretical curves. The second overflow tank in Figure 2 was used for the column experiments. The column was made of 2.4-cm-ID acrylic pipe, and the amount of adsorbent packed in the column was 10.9 cm^3. The velocity of seawater in the column was kept constant at 0.5 cm/s.

Adsorbent

Hydrous titanium oxide granulated with polyacrylonitrile (PAN-HTO) was used as the adsorbent. This adsorbent had

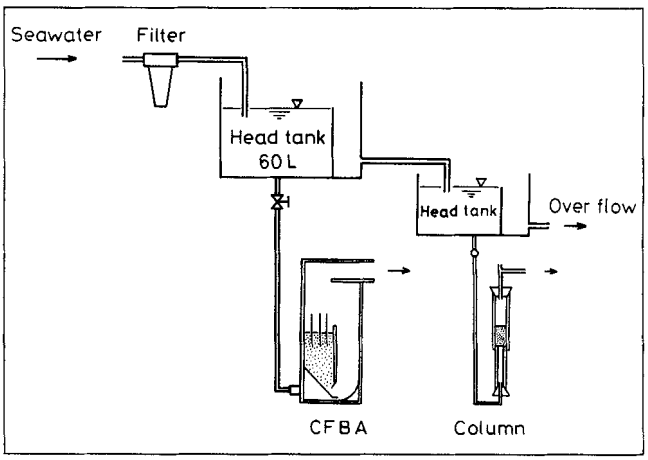

Figure 2. Adsorption experiment.

Table 1. Properties of PAN-HTO Adsorbent

Mesh	d_p (cm)	ρ_a (g/cm³) Dry	ρ_a (g/cm³) Wet	ρ_t (g/cm³)	ϵ_p
28/32	0.063	0.58	1.35	2.64	0.78
24/28	0.076	0.53	1.35	2.64	0.80
14/24	0.091	0.52	1.35	2.61	0.80

been used practically for recovering uranium from seawater in a test plant at the Nio Institute (Ogata, 1986).

This adsorbent consisted of hydrous titanium oxide particles of about 5 to 10 μm diameter. These fine particles were cross-linked with polyacrylonitrile to form larger particles. Its internal structure was porous (Nakamura et al., 1988). In the experiments, the PAN-HTO adsorbent was graded into three classes of mesh, 28/32, 24/28, and 14/24. Physical properties of the PAN-HTO adsorbent in each class are listed in Table 1.

Analysis of uranium uptake

At each prescribed time in the adsorption period, 2 cm³ of adsorbent particles was sampled from the CFBA in operation. The amount of uranium in the sample was determined by the following procedure.

(1) The sample was boiled in 6-N hydrochloric acid for one hour.

(2) The elutriant was passed at a constant flow rate through a column packed with anion exchange resin.

(3) Metal ions such as Mg^{++} and Ca^{++} were elutriated from the anion exchange resin by immersing into 6-N hydrochloric acid.

(4) Uranium ions were selectively elutriated from the anion exchange resin with 1-N hydrochloric acid.

(5) The concentration of uranium in the elutriant obtained in step 4 was determined by a fluorimetric method using an Aloka model FMT-4B fluorimeter.

The relative error in determining the concentration of uranium in natural seawater was 3% (Nakamura et al., 1988).

Experimental results

The amount of adsorbent that was carried over per day from the CFBA is plotted as a function of adsorption time in Figure 3. The value of u, which is a mean linear velocity of seawater, is derived by dividing the seawater flow rate F by the total area of the hole equipment, L times T. The seawater velocity in the contacting section is 2.5 times higher than u. A small amount of the adsorbent was carried through the experimental period. The carryover rate decreased with the adsorption time, t, and most of the adsorbent carried over was of very small particle size, which had not been removed from the original adsorbent in spite of grading. At the end of the experimental period of 144 hours, the ratio of the total adsorbent loss to the initial inventory was about 5% when $d_p = 14/24$ mesh and $u = 1.4$ cm/s. When $u = 0.9$ cm/s, the ratio reduced to about 0.7% in each mesh size.

The flow rate of seawater changed only slightly through the experimental period, and no adjustment of the head was needed to keep it constant. Even when unfiltered seawater was supplied

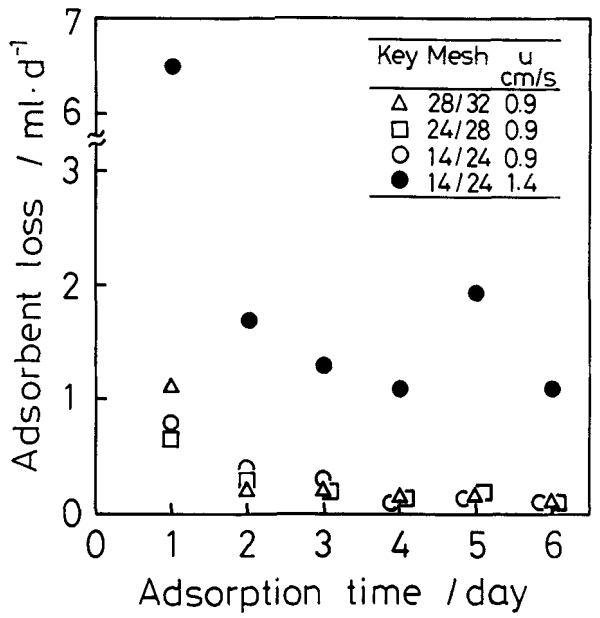

Figure 3. Daily amount of carried-over adsorbent as a function of adsorption time.

Seawater temperature is 13-17°C.

directly to the CFBA, the CFBA did not clog with the solids and weeds suspended in natural seawater. The CFBA ran very stably. Furthermore, there was little contamination of the adsorbent over the period of the experiment, and no decrease in the uranium uptake efficiency was observed (see Figure 4).

Figure 5 shows the influences of adsorbent particle size and mean linear velocity of seawater on the uranium uptake, q, per unit weight of the adsorbent. Seawater temperature was between 13 and 17°C. The broken line, dash-dotted line, and solid line in Figure 5 are numerical simulation results. These simulation results will be discussed later. The uranium ad-

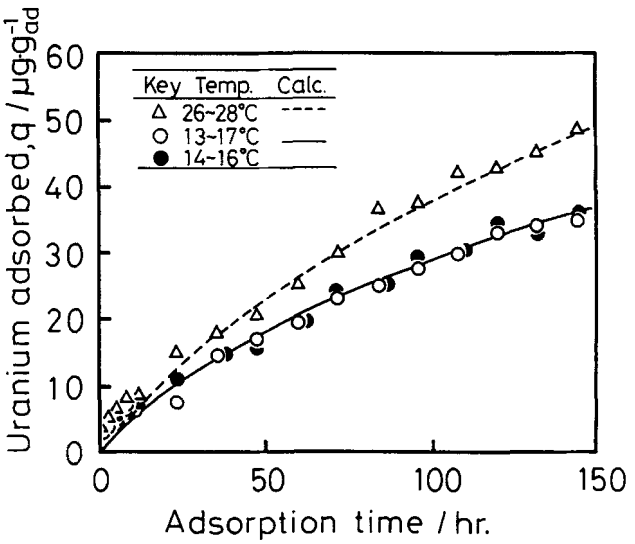

Figure 4. Dependence of uranium uptake on the seawater temperature.

Broken line and solid line are numerical simulation results. $d_p = 14/24$ mesh, $u = 0.9$ cm/s.

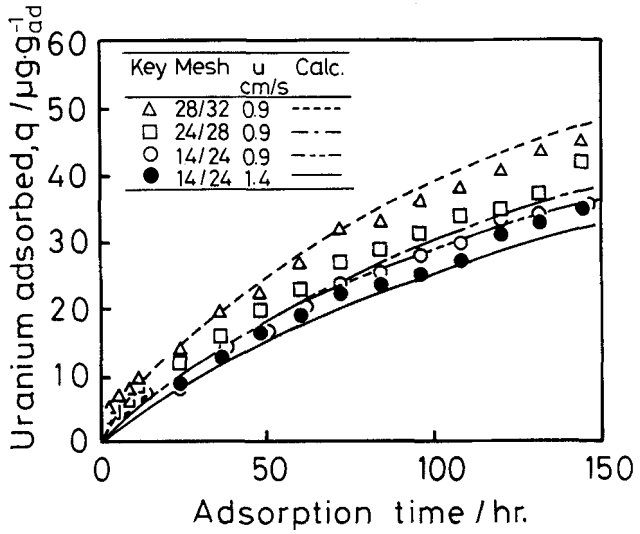

Figure 5. Influence of particle size and seawater velocity on the uranium uptake.

Broken line, dash-dotted line, and solid line are numerical simulation results. Seawater temperature is 13–17°C.

sorption rate of a small particle was greater than that of a large particle. Influence of the mean linear velocity of seawater on the uranium uptake was not distinct in this case.

Figure 6 shows the uranium recovery ratio R as a function of adsorption time, where R is the ratio of the quantity of uranium adsorbed to the quantity available in the seawater. The value of R decreased quickly in the early stage of the adsorption period, but soon the rate of decrease became small. At the end of the adsorption period of 144 hours, the uranium recovery ratios were 3 to 6%.

Seawater temperature was a very important factor in the recovery of uranium from seawater (Kanno and Saito, 1980). Dependence of uranium uptake on the seawater temperature

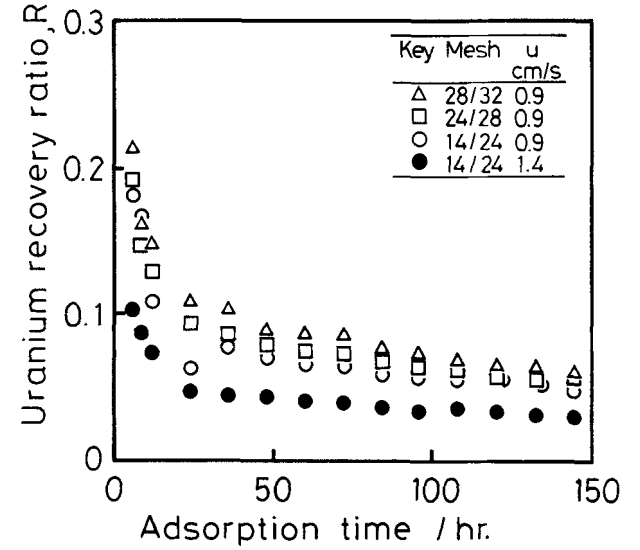

Figure 6. Uranium recovery ratio as a function of adsorption time.

Seawater temperature is 13–17°C.

is shown in Figure 4. The broken line and solid line in Figure 4 are numerical simulation results. The uranium adsorption rate was greater when the seawater temperature was higher. The experiments were carried out in different seasons, in the middle of May (○) and early in November (●). Seawater temperatures during these experiments were very close despite seasonal differences, so the uranium uptakes were almost equal. As mentioned above, unfiltered seawater was supplied directly to the CFBA in the experiment in November. However, a decrease of uranium uptake from the solids and/or contaminants suspended in seawater was not observed. This result proved that the uranium uptakes are equal if the seawater temperatures are equal, even though the experiments were carried out under different seawater conditions, filtered or unfiltered.

Numerical Simulation of Uranium Adsorption

Adsorption kinetic model

To predict the uranium adsorption performance of a plant-size CFBA, a numerical model simulating the adsorption kinetics in the CFBA was developed. In the numerical model, the overall movement of adsorbent particles was described by the following steps.

Step 1. At the start of operation, new adsorbent particles were loaded in the CFBA ($q=0$ at $t=0$).

Step 2. By supplying fresh seawater into the CFBA from the nozzle, the adsorbent particles mixed with the seawater and ascended in the contacting section. In this section, the adsorbent particles adsorbed the uranium ions in the seawater. The amount of uranium adsorbed in a particle gradually increased while ascending in the contacting section. In contrast, the concentration of uranium in the seawater gradually decreased while ascending in this section.

Step 3. The adsorbent particles were separated from the seawater in the upper part of the packing section and deposited there. In the packing section, the slip velocity between particles and seawater was small. Furthermore, the amount of uranium ions in the liquid phase between particles was very small in comparison with the adsorption capacity of the adsorbent. Thus, the uranium diffusion from the liquid phase to the particle surface was neglected in the packing section. In the particle, however, the uranium ions were transported inward by the concentration gradient of adsorbed uranium even when the particles move downward slowly in this section.

Step 4. Particles having already adsorbed some uranium in step 2 dropped through the slit (Particle nozzle section in Figure 1) and mixed again with fresh seawater.

Step 5. The adsorbent particles circulated continuously in the CFBA repeating from steps 2 to 4.

To treat the gradual change of uranium concentration in both seawater and particles in steps 2 and 3, the contacting section and packing section were divided into horizontal layers as shown in Figure 7. Equal amount of adsorbent was in each layer. No mixing of adsorbent between layers was assumed. The adsorbent particle was assumed to circulate in the CFBA stepwise, from no. 1 to no. 2 layer position, from no. 2 to no. 3, and so on for a residence time t_c. The residence time t_c, for which a certain layer of particles stays in a particular position, was defined by:

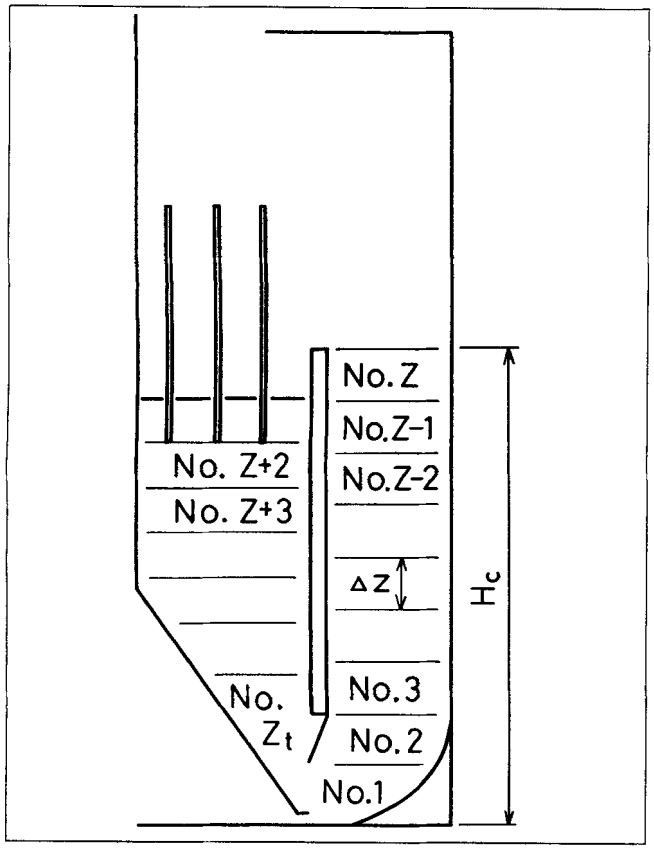

Figure 7. Modeling of the CFBA.

Contacting and packing sections are divided into layers, and the material balance is taken in each layer.

$$t_c = \frac{H_c}{(u_c - u_{ss})Z} \tag{1}$$

where u_c is the seawater velocity in the contacting section; u_{ss} is the settling velocity of the particle cluster, and $u_c - u_{ss}$, therefore, is rising velocity of the particle cluster.

With these assumptions, material balances were written as follows.

Material balance in a layer:

$$u_c \frac{\partial C}{\partial h} + k_f a_v (C - c_s) = \epsilon_b D_b \frac{\partial^2 C}{\partial h^2} \tag{2}$$

Diffusion in a particle:

$$D_e \left(\frac{\partial^2 c}{\partial r^2} + \frac{2}{r} \frac{\partial c}{\partial r} \right) = \rho_a \frac{\partial q}{\partial t} \tag{3}$$

Boundary condition:

$$\left(\frac{\partial c}{\partial r} \right)_{r=r_p} = \frac{\int_{Z_i}^{Z_{i+1}} k_f (C - c_s) dh}{D_e} \tag{4}$$

Initial condition:

$$q = c = 0 \quad (t = 0,\ 0 \le r \le r_p) \tag{5}$$

Freundlich-type adsorption isotherm:

$$\frac{q}{q_0} = \left(\frac{c}{C_0} \right)^{1/n} \tag{6}$$

where a_v is the particles surface area per unit volume of the contacting section, r is the radial position in the particle, c is the concentration of uranium at r, c_s is the concentration of uranium on the particle surface, C is the concentration of uranium in the liquid phase, C_0 is the uranium concentration in the seawater, D_b is the axial dispersion coefficient, D_e is the intraparticle diffusion coefficient, h is the height in the contacting section, k_f is the liquid-film mass-transfer coefficient, n is the Freundlich constant, q is the amount of uranium adsorbed at r, q_0 is the amount of uranium adsorbed in equilibrium with the C_0, r_p is the particle radius, t is the adsorption time, u_c is the seawater velocity in the contacting section, ϵ_b is the void fraction in the contacting section, and ρ_a is the apparent density of the adsorbent particle.

Parameters in the previous equations were determined by using D_b and k_f, which were calculated by Eqs. 7 and 8.

D_b (*Krishnaswamy et al., 1978*):

$$\left(1 - \sqrt{\frac{2D_b}{u_c H_c}} \right) \epsilon_b^{0.25} = 0.74 \tag{7}$$

k_f (*Shirozuka et al., 1987*):

$$k_f = \frac{ShD_v}{d_p} \tag{8}$$

where

$$Sh = \frac{(2 + 0.6 Re^{1/2} Sc^{1/3})}{\epsilon_b} \tag{9}$$

here d_p is the average particle size, D_v is the uranium diffusivity in seawater, H_c is the contacting section height, Re is the Reynolds number, Sc is the Schmidt number, Sh is the Sherwood number, and ν is the kinematic viscosity. D_v was taken from the data of Saito and Miyauchi (1981).

D_e was obtained from an experiment described in the next section. The adsorption isotherm of the PAN-HTO adsorbent was obtained from our previous batch experiments and could be represented by Freundlich's equation (Nakamura et al., 1988). The Freundlich constant n was 1.5, and q_0, which is the amount of uranium adsorbed in equilibrium with the uranium in natural seawater, 3.2 ppb, ranged from 103 to 149 μg/g, as shown in Table 2. Other parameters such as the particle radius, the particle density, and the seawater velocity were determined from previous independent measurements and/or experimental conditions.

Time dependence of uranium uptake in the CFBA was calculated by solving Eqs. 2 to 5 numerically with the Crank-Nicolson method.

Estimation of D_e

The intraparticle diffusion coefficient D_e was evaluated by comparing the experimental uranium uptake curve in the col-

Table 2. Intraparticle Diffusion Coefficient D_e and Adsorption Isotherm Parameters

Mesh	d_p (cm)	D_e (cm^2/s)	n^*	q_0^* (μg/g)	θ (°C)
28/32	0.063	1.4×10^{-6}	1.5	103	13-17
14/24	0.091	1.6×10^{-6}			
—	0.085	1.9×10^{-6}	1.5	114	18-22
14/24	0.091	2.2×10^{-6}	1.5	149	26-28

*Data taken from literature (Nakamura et al., 1988).

umn with theoretical curves following the method developed by Suzuki and Chihara (1982). The typical example of the curve fitting is shown in Figure 8, where τ is the dimensionless time defined as:

$$\tau = \left(\frac{D_e t}{r_p^2}\right)\left(\frac{C_0}{\rho_a q_0}\right) \tag{10}$$

Open circles represent the experimental data: $d_p = 14/24$ mesh, $u = 0.5$ cm/s, and seawater temperature 26-28°C. The theoretical curve of q/q_0 vs. τ was obtained by solving numerically a set of diffusion equations for the column. The two parameters in this figure are the Freundlich constant, n, and the Biot number, Bi', defined as:

$$Bi' = \frac{r_p^2}{D_e}\left(\frac{1}{\frac{r_p}{k_f} + \frac{3W_{ad}}{\rho_a F}}\right) \tag{11}$$

where W_{ad} is the adsorbent inventory, and Bi' is a ratio of k_f and D_e, which represents the rate-determining step of uranium adsorption. The uranium adsorption process is intraparticle, which is diffusion-controlled when $Bi' = \infty$ and liquid-film mass-transfer controlled when $Bi' = 0$. In our case, the experimental data are fitted best by a theoretical curve with $Bi' = 20$. This suggests that the rate-determining step of uranium adsorption is under the control of the intraparticle diffusion rate rather than the liquid-film mass-transfer rate. In this case, the dimensionless time τ of 0.01 corresponds to the real adsorption time t of 66 hours. Therefore, D_e is obtained by Eq. 10 as $D_e = 2.2\times10^{-6}$ cm^2/s.

The values of D_e evaluated from the curve fitting are shown in Table 2; D_e is independent of the particle size, but increases with seawater temperature.

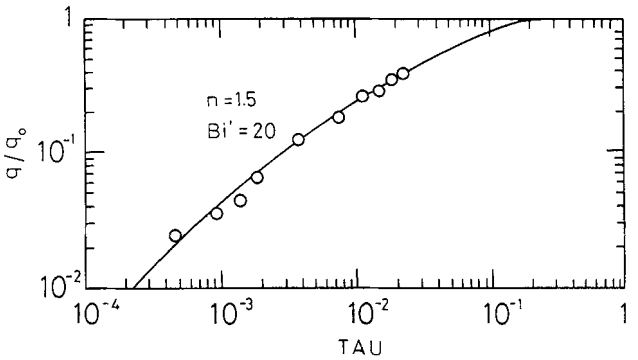

Figure 8. Curve fitting of the column experiment to the theoretical curve.

Open circles represent the experimental data: $d_p = 14/24$ mesh, $u = 0.5$ cm/s, and seawater temperature = 26-28°C.

Results of numerical simulation

Among the parameters in the basic equations of material balances (Eqs. 2-6), d_p, ρ_a, ϵ_b, and u_c were determined from the experimental conditions. D_e was obtained from the column experiments as described in the previous section. Other parameters, D_b and k_f, were calculated by substituting the experimental conditions for Eqs. 7 and 8.

Curves obtained by the numerical simulation are shown in Figures 4 and 5. The broken line, dash-dotted line and solid line are numerical simulation results. The numerical simulation results are in good agreement with the experimental data over the whole adsorption period. The adsorption kinetic model was confirmed to be reliable. It should be noted that all parameters in the numerical calculation are determined experimentally and no adjustable parameter was used. These parameters are listed in Table 3.

In the numerical calculation, the contacting section was divided into Z unit layers to treat gradual changes in the uranium concentration in that section. Z was changed from 1 to 30 in our calculation. The uranium recovery ratio in the present experiments, however, was low, and the concentration gradient of the uranium in the contacting section was small. Therefore, the bed division number Z did not affect calculated results significantly in this case.

Discussion

The uranium adsorption rate from the liquid phase to the particle surface, N_a, is expressed as:

Table 3. Parameters Used in the Numerical Calculation*

	Calc.	d_p (cm)	u (cm/s)	D_e (cm^2/s)	n	q_0 (μg/g)	H_c (cm)	W (cm^3)	θ (°C)
Fig. 4	- - - - -	0.063	0.9	1.4×10^{-6}	1.5	103	15	275	13-17
	— - —	0.076	0.9	1.4×10^{-6}					
	— - - —	0.091	0.9	1.6×10^{-6}					
	———	0.091	1.4	1.6×10^{-6}					
Fig. 6	- - - - -	0.091	0.9	2.2×10^{-6}	1.5	149	15	275	26-28
	———	0.091	0.9	1.6×10^{-6}	1.5	103	15	275	13-17

*D_b and k_f were calculated by substituting the experimental conditions for Eqs. 7 and 8.

$$N_a = k_f a_v (C - c_s) \tag{12}$$

and a_v is expressed by:

$$a_v = \frac{6(1-\epsilon_b)}{d_p} \tag{13}$$

Thus, the uranium adsorption rate increases with decreasing adsorbent particle size, as shown in Figure 5. The smaller the particles of adsorbent, the more effective is the recovery of uranium. The settling velocity of an adsorbent particle, however, becomes small with decreasing adsorbent particle size. Smaller adsorbent particles are carried over more easily than larger ones. Thus, the working velocity region, in which the adsorbent particles circulate well in the CFBA without deposition and carryover, becomes lower and narrower as the particles become smaller (Nakamura et al., 1990). The appropriate adsorbent particle size should be determined from the viewpoints of both the adsorption rate and the working velocity region.

The influence of mean linear velocity of seawater on the uranium uptake is not distinct, as shown in Figure 5. In the operation of the CFBA, the concentration of adsorbent particles suspended in the contacting section decreases at higher seawater velocity. Therefore, the amount of adsorbent in the packing section increases with the increase in the seawater velocity, and the time during which the particles move downward slowly in this section becomes longer. Thus, the net contacting time between fresh seawater and the adsorbent in the contacting section decreases with the increase in the seawater velocity. This is unfavorable to the uranium uptake. The liquid-film mass-transfer rate between the liquid phase and the particle surface, however, increases with the increase in the seawater velocity as expressed in Eqs. 8 and 9. This is favorable to the uranium uptake. We consider that the influence of the seawater velocity on the uranium uptake is not distinct because of these two opposite influences.

Adsorbent particles stay in the packing section for a considerable portion of total adsorption period. They slowly move downward, and their presence prevents a backward flow of freshly supplied water (Nakamura et al., 1990). We assumed that the uranium adsorption is negligible, but the intraparticle transport of uranium took place in the packing section. We estimated the contribution of the intraparticle transport to the uranium uptake by calculating for the following three cases and compared them with experimental data to verify our assumption.

Case 1. Deposition time in the packing section is assumed to be zero (broken line in Figure 9).

Case 2. Deposition time is taken into account as an idle period; the intraparticle transport of uranium does not occur in the packing section (dash-dotted line in Figure 9).

Case 3. Intraparticle transport of uranium takes place during the deposition time, that is, the adsorption front of uranium in an adsorbent particle moves inward, while the particle stays in the packing section (solid line in Figure 9). The simulation result of case 3 is in good agreement with the experimental data represented by open circles.

In the packing section, the diffusion of uranium from the liquid phase to the particle surface is negligible, so the uranium concentration on the particle surface decreases by the inward

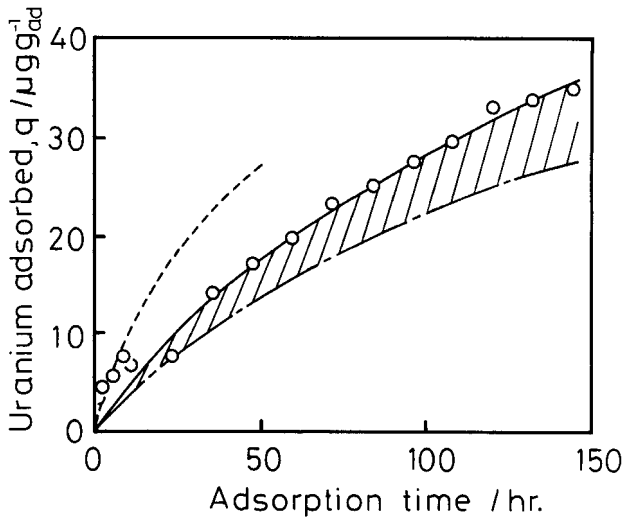

Figure 9. Contributions of contacting and packing sections to the uranium uptake.

Open circles represent the experimental data: $d_p = 14/24$ mesh, $u = 0.9$ cm/s, and seawater temperature = 13–17°C. Broken line is case 1, dash-dotted line case 2, and solid line case 3. Dash-dotted line shows the uranium uptake in the contacting section. The shaded region shows the effect of intraparticle transport of uranium in the packing section.

movement of the adsorption front. The decrease in uranium concentration on the surface region is favorable for uranium adsorption in the contacting section at the next circulation, because the uranium diffusion rate from the liquid phase to the particle surface is proportional to the concentration gradient on the liquid-film boundary, as expressed in Eq. 12. Since the dash-dotted line in the Figure 9 shows the uranium uptake in the contacting section, the region denoted by the shaded area shows the effect of the intraparticle transport of uranium in the packing section.

The uranium recovery ratio in the CFBA was 3 to 6% at the end of adsorption period of 144 hours. As the adsorption of uranium from seawater takes place mainly in the contacting section, the contacting section height must be increased to recover significant amounts of uranium from seawater. We have examined modified and scaled-up CFBA's and achieved the recovery ratio of 10% or more. The performance comparable to a conventional fluidized bed could be obtained in these beds (Ito et al., 1991). Excessive increase in the contacting section height, however, causes the increase in pressure drop through the bed (Nakamura et al., 1990). Thus, the contacting section height should be designed considering both the uranium adsorption rate and the energy consumption to the force transporting the seawater.

Conclusions

Recovery of uranium from natural seawater was carried out using a small CFBA to investigate its adsorption characteristics. Hydrous titanium oxide granulated with polyacrylonitrile was used as the adsorbent.

The CFBA ran stably with small loss of adsorbent over the period required by the adsorbent to collect a practical amount of uranium. Neither clogging nor change of the flow rate

occurred during the period even when unfiltered seawater was supplied to the CFBA.

The important advantage of the CFBA is that no distributor is required to hold adsorbent particles. This is worth noting because any filter or distributor inevitably gathers solids and /or weeds suspended in seawater during a long period of operation, and some protection against this is needed for conventional beds.

The uranium uptake increased with decreasing adsorbent particle size and increasing seawater temperature. The numerical model proposed in this study simulated well the adsorption kinetics in the CFBA. The model will be useful for improvement of the adsorption ability of the CFBA and for the design of a plant-size CFBA.

We consider that the CFBA is one of the best solutions at the present stage for the problem of recovering uranium from seawater.

Acknowledgment

This study was supported by Grant-in-Aid of Scientific Research of the Ministry of Education, Science and Culture, Japan, No. 63603006. The authors would like to thank Messrs. T. Oba and K. Iwafuchi, students of the Department of Mechanical Engineering, Nagaoka University of Technology, for their assistance in the experiments. We are grateful to the Metal Mining Agency of Japan, for supplying PAN-HTO adsorbent. Prof. Y. Honma and the staff at Sado Marine Biological Station of Niigata University are also acknowledged for their support, as well as the reviewers for their helpful comments.

Notation

a_v = particles surface area per unit volume of contacting section, cm^2/cm^3
Bi' = Biot number, Eq. 11
c = concentration of uranium with radial position r in particle, $\mu g/L$
c_s = concentration of uranium on particle surface, $\mu g/L$
C = concentration of uranium in liquid phase, $\mu g/L$
C_0 = uranium concentration in seawater, $\mu g/L$
d_p = average particle size, cm
D_b = axial dispersion coefficient, cm^2/s
D_e = intraparticle diffusion coefficient, cm^2/s
D_v = uranium diffusivity in seawater, cm^2/s
F = flow rate of seawater, cm^3/s
h = axial position in contacting section, cm
H = bed height, cm
H_c = contacting section height, cm
k_f = liquid-film mass-transfer coefficient, cm/s
L = bed width, cm
L_c = contacting section width, cm
L_s = packing section width, cm
n = Freundlich constant
N_a = uranium adsorption rate from liquid phase to particle surface, $\mu g/L \cdot s$
q = amount of uranium adsorbed with radial position r in particle, $\mu g/g$
q_0 = amount of uranium adsorbed in equilibrium with C_0, $\mu g/g$
r = radial position in particle, cm
r_p = particle radius, cm
Re = Reynolds number, $u_c d_p/\nu$
Sc = Schmidt number, ν/D_v
Sh = Sherwood number, $k_f d_p/D_v$
t = adsorption time, s
T = bed thickness, cm
t_c = residence time over which a certain amount of particles stay in a layer contacted with seawater, s
u = mean linear velocity of seawater $= F/L \cdot T$, cm/s
u_c = seawater velocity in contacting section $= F/L_c \cdot T$, cm/s
u_s = settling velocity of an adsorbent particle, cm/s
u_{ss} = settling velocity of adsorbent particles cluster, cm/s
W = adsorbent inventory, cm^3
W_{ad} = adsorbent inventory, g
Z = number of adsorbent layers in contacting section
Z_t = total number of adsorbent layers
ΔZ = thickness of unit adsorbent layer

Greek letters

ϵ_b = void fraction in contacting section
ϵ_p = adsorbent porosity
θ = seawater temperature, °C
ν = kinematic viscosity, cm^2/s
ρ_a = apparent density of adsorbent particle, g/cm^3
ρ_t = true density of adsorbent particle, g/cm^3
τ = dimensionless time, Eq. 10

Literature Cited

Ito, Y., S. Nakamura, S. Yoshimuta, M. Shirakashi, and M. Kanno, "Development of a Circulating Fluidized Bed Adsorber for Recovery of Uranium from Seawater," *Proc. ASME-JSME Fluids Eng. Conf.*, Liquid-Solid Flows, FED-Vol. 118, Portland, OR, 207 (1991); S. Nakamura, Y. Ito, K. Iwafuchi, and M. Shirakashi (to be submitted).

Kanno, M., and K. Saito, "Recovery of Uranium from Seawater," *Proc. Topical Meeting on Recovery of Uranium from Seawater*, MIT-EL-80-031, 149 (Dec., 1980).

Kanno, M., "Present Status of Study on Extraction of Uranium from Seawater," *J. Nucl. Sci. Technol.*, **21**, 1 (1984).

Koske, P. H., and K. Ohlrogge, "The Adsorber Loop Concept for the Contact between Seawater and Adsorber Granulate," *Proc. Int. Meeting on Recovery of Uranium from Seawater*, Tokyo, 68 (Oct. 17–19, 1983).

Krishnaswamy, P. R., R. Ganapathy, and L. W. Shemilt, "Correlating Parameters for Axial Dispersion in Liquid Fluidized Systems," *Can. J. Chem. Eng.*, **56**, 550 (1978).

Nakamura, S., Y. Ito, and M. Kanno, "The Influence of Adsorbent Properties on Uranium Recovery Cost," *Nihon Kaisui Gakkaishi*, **41**, 38 (1987).

Nakamura, S., S. Mori, S. Yoshimuta, Y. Ito, and M. Kanno, "Uranium Adsorption Properties of Hydrous Titanium Oxide Granulated with Polyacrylonitrile," *Sep. Sci. Technol.*, **23**, 731 (1988).

Nakamura, S., S. Yoshimuta, M. Shirakashi, M. Kanno, and Y. Ito, "Development of a Circulating Fluidized Bed Adsorber," *AIChE J.*, **36**, 1003 (1990).

Ogata, N., "Nio Institute on Uranium Recovery from Seawater," *Nihon Kaisui Gakkaishi*, **40**, 247 (1986).

Saito, K., and T. Miyauchi, "Diffusivities of Uranium in Artificial Seawater," Kagaku Kogaku Ronbunshu, **7**, 545 (1981).

Shirozuka, T., A. Hirata, and A. Murakami, "Idou Sokudo Ron," *Omusha*, 241 (1987).

Suzuki, M., and K. Chihara, "Adsorption Uptake in a Shallow Bed Adsorber," *Seisan-Kenkyu*, **34**, 149 (1982).

Manuscript received Oct. 31, 1991, and revision received Mar. 25, 1992.